MU-MIMO in LTE Systems

Duplicy, Jonathan; Badic, Biljana ; Balraj, Rajarajan ; Ghaffar, Rizwan ; Horvath, Peter ; Kaltenberger, Florian ; Knopp, Raymond ; Z. Kovacs, Istvan ; Nguyen, Hung Tuan; Tandur, Deepaknath ; Vivier, Guillaume

Published in:
EURASIP Journal on Wireless Communications and Networking

DOI (link to publication from Publisher):
10.1155/2011/496763

Publication date:
2011

Document Version
Early version, also known as pre-print

MU-MIMO in 4G systems

Jonathan Duplicy, Biljana Badic, RajaRajan Balraj, Rizwan Ghaffar, Péter Horváth, Florian Kaltenberger, Raymond Knopp, István Z. Kovács, Hung T. Nguyen, Deepaknath Tandur and Guillaume Vivier

***Abstract*—This article first presents an overview of the different MU-MIMO schemes included / being studied in 3GPP standardization; from LTE to LTE-Advanced. Various receiver architectures are then studied and their performance assessed through link-level simulations. Appealing performance increase offered by interference aware receiver is notably emphasized. Furthermore, system level simulations for LTE Release 8 are provided. Interestingly, it is shown that MU-MIMO only offers marginal performance gains with respect to single-user MIMO. This arises from the limited MU-MIMO features included in Release 8 and calls for improved schemes for the upcoming releases.**

***Index Terms*—MIMO, Multi-User, 4G, LTE, LTE-Advanced.**

I. Introduction

Thanks to the success of smarthpones and mobile-ready portables, such as laptops or tablets mobile data traffic has recently experienced an exponential growth [1]. The demand for mobile data services has increased by an average of 160% in the year 2009 alone and some mobile carriers have experienced even more aggressive growth numbers. According to a recent forecast, the global mobile data traffic is expected to continue to double every year through 2014, leading to a global compound annual growth rate of 108% [2].

These large capacity demands can be met only by highly efficient and optimized mobile network infrastructures. Significant improvements are expected with the ongoing roll-out of OFDMA (Orthogonal Frequency Division Multiple Access) -based networks: WiMAX and LTE. These two standards, although do not fulfill the requirements, are the first steps towards the 4G definition given by ITU (International Telecommunications Union) and targeting data rates of 100Mbps in high mobility applications and 1Gbps for low mobility applications such as nomadic / local wireless access.

To meet these needs, advanced features are investigated for inclusion in the future releases of these standards (WiMAX Evolution and LTE-Advanced). Among these various techniques, two promising ones are currently investigated by the EU FP7 project SAMURAI (Spectrum Aggregation and Multi-User MIMO: ReAl-World Impact), namely carrier aggregation and Multi-User MIMO (MU-MIMO).

In this article, the SAMURAI consortium presents first (Section II) a critical overview of the different MU-MIMO schemes included / being studied in 3GPP releases; from LTE Release 8 to Release 10 (LTE-Advanced). In addition, we propose a new scheduling algorithm based on the geometrical alignment of interference at the base station which relegates the effective interference seen by each user equipment (UE).

In Section III, receiver design is addressed. Several receiver structures are analyzed and their performance compared. Among others, an interference aware receiver showing appealing performance gains is studied.

Finally, system level simulations are provided in Section IV. Gains offered by MU-MIMO schemes with respect to SU-MIMO schemes in LTE Release 8 are notably emphasized.

Regarding notations, we will use lowercase or uppercase letters for scalars, lowercase boldface letters for vectors and uppercase boldface letters for matrices. Furthermore, $|\cdot|$, $\|\cdot\|$ and $\|\cdot\|_F$ indicate the norm of scalar, vector and Frobenius norm of a matrix while $(.)^T$, $(.)^*$ and $(.)^\dagger$ stand for the transpose, conjugate and conjugate transpose, respectively.

II. Overview of MU-MIMO in 3GPP standards

A. Theoretical foundations of MU-MIMO

Spatial dimension surfacing from the usage of multiple antennas promises improved reliability, higher spectral efficiency and spatial separation of users. This spatial dimension is particularly beneficial for precoding in the downlink of multi-user (MU) cellular system, where spatial resources can be used to transmit data to multiple users simultaneously. The MIMO transmission techniques are integral parts of the LTE and WiMAX standards. A good overview of the MIMO techniques and configuration supported in these radio access technologies can be found in [3], [4], [5], [6].

In MU-MIMO mode the transmissions to several terminals are overlapped in the same time-frequency resources by exploiting the spatial diversity of the propagation channel. In order to fully exploit MU-MIMO transmission modes the spatial streams intended to the targeted terminals need to be well separated, ideally orthogonal at both transmit and receive sides. As a consequence, the theoretical performance gain of the MU-MIMO over SU-MIMO are expected to significantly increase in spatially correlated channels and with increasing number of transmit antenna at the Enhanced NodeB (eNB). Various linear and non-linear precoding techniques and the

Jonathan Duplicy (contact author) and Deepaknath Tandur are with Agilent Technologies Laboratories, Wingepark 51, 3110 Rotselaar, Belgium; jonathan_duplicy@agilent.com, deepaknath_tandur@agilent.com

Biljana Badic and RajaRajan Balraj are with Infineon Technologies AG, Düsseldorfer Landstrasse 401,47259 Duisburg, Germany; Biljana.badic@infineon.com

Rizwan Ghaffar, Florian Kaltenberger and Raymond Knopp are with Eurecom, 2229 route des Crêtes, B.P.193, 06904 Sophia Antipolis Cedex, France; rizwan.ghaffar@eurecom.fr, florian.kaltenberger@eurecom.fr, raymond.knopp@eurecom.fr

Péter Horváth is with the Dept. of Broadband Infocommunications, Budapest University of Technology and Economics, 1111 Goldmann Gy. ter 3., Budapest, Hungary; hp@hvt.bme.hu

István Z. Kovács is with Nokia Siemens Networks Denmark A/S, Niels Jernes Vej 10, DK9220, Aalborg, Denmark; istvan.kovacs@ieee.org

Hung Tuan Nguyen is with Department of Electronics Systems Aalborg University, Niels Jernes Vej 12, DK9220, Aalborg, Denmark; htn@es.aau.dk

Guillaume Vivier is with Sequans Communications, Le Parvis de la Défense 19, 92 073 Paris La Défense Cedex, France; gvivier@sequans.com

corresponding receiver structures have been proposed in the literature in order to achieve promising MU-MIMO gains, e.g. [7], [8], [9], [10], [11].

Optimal precoding in MU-MIMO Gaussian broadcast channel involves a theoretical pre-interference subtraction technique known as dirty paper coding (DPC) [9] combined with an implicit user scheduling and power loading algorithm. Linear precoding techniques as channel inversion (CI) [10] and regularized channel inversion (RCI) [11] cancel the interference in the former case while attenuate it in the latter case. These precoding strategies strive to transform the cross-coupled channels into parallel noninteracting channels therefore transforming MU downlink into parallel single-user (SU) systems. However they do not exploiting the knowledge of the interference structure to mitigate its effects. This evasion is evident as these precoding strategies are based on the Gaussian assumption for interference which encompasses no structure to be manipulated. However in the real world, inputs must be drawn from discrete constellations which have structures that can be exploited in the detection process.

For practical purposes, the found theoretical solutions have to be further adapted to the requirements and restrictions of standardized air-interfaces. The following sections summarize some of the critical physical layer design aspects.

B. Overview of 3GPP LTE PHY MIMO

1) Reference signals: The downlink transmission schemes are supported at physical layer by a set of downlink reference signals. These reference signals can be either UE specific or cell specific. The latter are referred to as common reference signals (CRS) while the former are referred to as dedicated (demodulation) reference signals (DRS or DM-RS). The CRS are not precoded signals and are used by the UE for channel estimation, while the DM-RS are precoded and used for demodulation purposes on the scheduled physical resources blocks (PRB). The 3GPP standard define the transmission of one time-frequency pattern for CRS and DM-RS assigned to one real or virtual *antenna port*.

2) Transmission modes: The defined SIMO and MIMO transmission schemes are categorized in several *transmission modes*. The definition of each transmission mode includes the required configuration information in the common downlink signaling channel and information on how the user terminal should search for this configuration message [12]. This mechanism is part of the general downlink signaling framework designed to allow a flexible time-frequency resource allocation separately to each UE based on the available system resources and the reported or measured channel conditions. The transmission mode for each UE is configured semi-statically via higher layer signaling, in order to avoid excessive downlink signaling.

3) Precoding: A major pre-requisite for SU- and MU-MIMO transmission schemes is the use of precoding mechanisms at the transmit side. In 3GPP LTE / LTE-Advanced different codebooks have been defined depending on the number of transmit antenna ports and they provide precoding support for simultaneous transmission of variable number of layers (data stream) to the same target UE [3], [4], [5], [6], [12].

The precoding is applied to the data transmission to a target UE based on the channel feedback received from that UE, including a channel rank indicator (RI), channel quality indicator (CQI) and precoding matrix indicator (PMI). The RI indicates the estimated number of simultaneous layers which can be received by the UE. One or more layers can be mapped to the same *codeword* and are jointly encoded for transmission to the same target UE. The RI is estimated at the UE as a wideband measure i.e., the same channel rank is assumed on all allocated resources. The CQI is an index in the modulation coding scheme (MCS) and transport block size (TBS) index table (32 different entries). The PMI is an index in the codebooks defined for a given number or transmit antenna ports (1, 2, 4 in LTE and up to 8 for LTE-Advanced). The CQI information is always derived under the assumption that the selected PMI will be applied to the next scheduled transmission. A more detailed analysis of the LTE MU-MIMO precoding mechanisms and codebook use is presented in Section II-C2.

4) Signalling and terminal feedback: The physical layer procedures defined for LTE Release 8 support various mechanisms of controlling the transmission parameters with both higher layer and lower layer signaling [12], [13]. The time-frequency granularity of the feedback to be sent by the UE is configured by the network via the downlink signaling channel and scheduling grants. Certain restrictions apply mainly due to requirement of minimizing the downlink and uplink signaling overheads and in practice this means that each of the defined *transmission modes* supports a certain limited set of physical layer transmission schemes and feedback schemes.

There are two main categories of CQI / PMI feedback mechanisms defined in the time-domain: periodic and aperiodic. The RI is always a frequency non-selective type feedback and is associated with the corresponding CQI / PMI feedback. The supported time-frequency CQI / PMI feedback granularities determine the overall feedback amount, and the supported configurations depend on the physical uplink channel utilized. The aperiodic feedback - frequency selective - is supported on the uplink shared channel and is available only when the UE has downlink / uplink transmission scheduled while for the periodic feedback - frequency non / selective - both uplink control and shared channels can be used [12].

C. Downlink MU-MIMO in LTE

1) LTE Release 8: The first release of LTE (Release 8) was aimed at defining the new OFDMA based air-interface and introduced advanced single-user MIMO transmission schemes, which were evaluated to be sufficient to meet the set performance targets [3], [4], [5], [6], [14]. Transmission from up to four antenna ports is supported. The spatial multiplexing or diversity MIMO transmission schemes, i.e. including MU-MIMO, use only the non-precoded CRS while the pre-

TABLE I
CQI AND PMI FEEDBACK TYPES FOR TRANSMISSION MODE 5 IN LTE

Mode	CQI type	PMI type
Aperiodic	Higher-layer configured, set of sub-bands: Subband and Wideband CQI per codeword	Single PMI
Periodic	Wideband CQI for first codeword Spatial differential CQI for $\mathrm{RI} > 1$	Single PMI
Periodic	UE selected subbands: Full CQI for first codeword Spatial differential CQI for $\mathrm{RI} > 1$	Single PMI

coded DRS can support single-user single-layer beam-forming schemes.

In LTE Release 8 there is only one transmission mode defined which allows for MU-MIMO scheme to be used, the *transmission mode 5* (TM5). When configured in TM5, the UE assumes that the eNB transmission on the downlink shared channel is performed with a single layer (stream). Furthermore, the downlink control information includes a 1-bit power offset information, indicating whether a 3 dB transmit power reduction should be assumed or not.

In terms of terminal feedback and CQI / PMI reporting modes, the LTE MU-MIMO transmission mode 5 can use both aperiodic and periodic feedback types, see Table I. When aperiodic reporting is configured then the wideband CQI and higher layer selected subband CQI in combination with a single PMI is supported. The full CQIs are reported for each codeword. When periodic reporting is configured then either wideband CQI or UE selected subband CQI in combination with a single PMI is supported. The full CQI is reported for the first codeword only and differential CQI is used for the second codeword when the reported $\mathrm{RI} > 1$. Single (or wideband) PMI means that the reported PMI corresponds to, and assumes transmission on, all selected subbands reported for the CQI(s) and RI.

This is a rather minimal MU-MIMO transmission scheme and relies heavily on the accuracy of the RI / CQI / PMI feedback which was optimized for SU-MIMO transmission schemes. Inevitably this limits the achievable MU-MIMO performance.

2) Signal Model: The precoders defined in LTE [15] are low resolution and are based on the principle of equal gain transmission (EGT). The efficient employment of these precoders for MU-MIMO mode is not yet fully understood. This has led to the common perception that MU-MIMO is not workable in LTE [16] (page 244). It was shown in [7] that MU-MIMO mode performs better than SU-MIMO mode when spatial correlation is assumed at the transmit side. In this section, we investigate the effectiveness of these low resolution precoders for MU-MIMO mode in LTE and propose a geometric scheduling algorithm which outperforms MIMO and transmit diversity schemes. This algorithm is based on the geometrical alignment of interference at eNB which relegates the effective interference seen by each UE. The residual interference is still significant and can be exploited in the detection process. To this end, we propose the employment of a matched filter (MF) based low complexity interference aware receiver which not only reduces one complex dimension of the system but also exploits the interference structure in the detection process.

For the case of eNB with two antennas (baseline configuration of LTE), the standard specifies the use of four precoders based on two bits feedback from the UEs which are given as $[1 \quad q]^T$ where $q \in [\pm 1, \pm j]$. The number of precoders increases to sixteen in the case of four transmit antennas however in this section we restrict to the case of two transmit antennas. System equation for LTE mode 5 at the k-th resource element (RE) for single antenna UEs is given as

$$y_{1,k} = \mathbf{h}_{1,k}^{\dagger}\mathbf{p}_{1,k}x_{1,k} + \mathbf{h}_{1,k}^{\dagger}\mathbf{p}_{2,k}x_{2,k} + z_{1,k}$$

where $y_{1,k}$ is the received symbol at UE-1 and $z_{1,k}$ is zero mean circularly symmetric complex white Gaussian noise of variance N_0. $x_{1,k}$ and $x_{2,k}$ are the complex symbols for UE-1 and UE-2 respectively. $\mathbf{h}_{1,k}^{\dagger} = [h_{11}^* \quad h_{21}^*]$ symbolizes the spatially uncorrelated flat Rayleigh fading MISO channel from eNB to UE-1 at the k-th RE. Since the processing at UE is assumed to be performed on a RE basis for each received OFDM symbol, the dependency on RE index can be ignored for notational convenience.

Our proposed precoding strategy involves computation of low complexity matched filter (MF) precoder at UEs. As the decision to schedule a UE in SU-MIMO, MU-MIMO or transmit diversity mode will be made by eNB, so each UE would feedback the precoder which maximizes its received signal strength. Therefore, in accordance with the low resolution LTE precoders, the UEs compute quantized versions of their respective MF precoders i.e. UE first measures its channel $\mathbf{h}_1^{\dagger} = [h_{11}^* \quad h_{21}^*]$ from eNB and consequently computes the MF precoder i.e. $[h_{11} \quad h_{21}]^T$ (the normalized version involves a division by $\|\mathbf{h}_1\|$). As LTE precoders are characterized by unit coefficients as their first entry, UE normalizes first coefficient of the MF precoder, i.e.

$$\mathbf{p}_{MF} = \frac{h_{11}^*}{|h_{11}|^2}\begin{bmatrix} h_{11} \\ h_{21} \end{bmatrix} = \begin{bmatrix} 1 \\ h_{11}^* h_{21} / |h_{11}|^2 \end{bmatrix} \qquad (1)$$

Second coefficient indicates the phase between two channel coefficients. Now based on the minimum distance between $\mathbf{p}_{MF}$ and LTE precoders, one of the four precoders is selected by the UE and the index of that precoder is fed back to eNB. Let that precoder be $\mathbf{p}_1 = [1 \quad q]^T, \quad q \in [\pm 1, \pm j]$. From the geometrical perspective, this precoder once employed by the eNB would align h_{21}^* with h_{11}^* in the complex plane so as to maximize the received signal power i.e. $|h_{11}^* + q h_{21}^*|^2$ subject to the constraint that the precoder allows rotation of h_{21}^* by $0°, \pm 90°$ or $180°$. Therefore this precoding ensures that h_{11}^* and h_{21}^* lie in the same quadrant as shown in Fig. 1(b). eNB may employ the requested precoders if it decides to serve the UE in SU-MIMO mode (transmission mode 6).

3) Optimal Precoding Strategy: In MU-MIMO mode, eNB can serve two UEs on the same time-frequency resources. We assume a densely populated cell where eNB has the requested precoders of most of the UEs in the cell. Here we propose a scheduling algorithm for MU-MIMO mode where eNB selects the second UE in each group of allocatable RBs

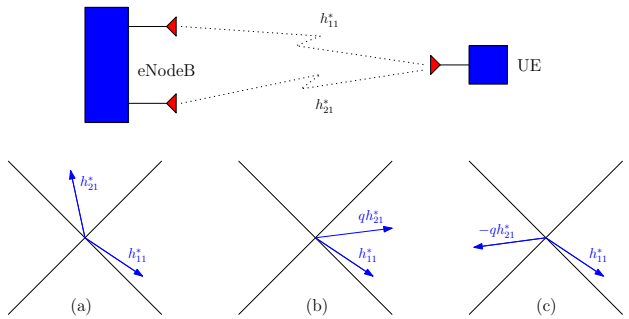

Fig. 1. (a) shows the original channel from eNB to UE while (b) shows the effective channel of desired signal while (c) shows the effective channel of interference of UE.

whose requested precoder $\mathbf{p}_2$ is $180°$ out of phase from the precoder $\mathbf{p}_1$ of the first UE to be served on the same RBs i.e. the precoder matrix is given as $\mathbf{P} = \frac{1}{\sqrt{4}} \begin{bmatrix} 1 & 1 \\ q & -q \end{bmatrix}$. So the received signal by UE-1 is given as

$$y_1 = \frac{1}{\sqrt{4}} \left(h_{11}^* + qh_{21}^*\right) x_1 + \frac{1}{\sqrt{4}} \left(h_{11}^* - qh_{21}^*\right) x_2 + z_1 \quad (2)$$

where selection of the precoder for each UE would ensure maximization of its desired signal strength i.e. $\left|\mathbf{h}_1^\dagger \mathbf{p}_1\right|^2$ for the first UE and $\left|\mathbf{h}_2^\dagger \mathbf{p}_2\right|^2$ for the second UE while selection of the UE pairs with out of phase precoders would ensure minimization of interference strength seen by each UE i.e. $\left|\mathbf{h}_1^\dagger \mathbf{p}_2\right|^2$ for the first UE and $\left|\mathbf{h}_2^\dagger \mathbf{p}_1\right|^2$ for the second UE. Note that this maximization and minimization is subject to the constraint of the utilization of low resolution LTE precoders. This scheduling strategy would ensure that the UEs selected to be served in MU-MIMO mode on same time-frequency resources have good channel separation.

Though this precoding and scheduling strategy would ensure minimization of interference under the constraint of low resolution LTE precoders, the residual interference would still be significant. The employment of single-user receivers by the UEs thereby assuming residual interference to be Gaussian would be highly suboptimal. In the sequel of the article, we will deliberate on a low complexity interference aware receiver which on one hand reduces one complex dimension of the system while on the other, exploits interference structure in the detection of desired stream.

D. LTE Release 9

In the second release of LTE (Release 9) new support has been added for the transmission modes utilizing virtual antenna ports with precoded UE-specific reference signals. The DRS has been extended to two additional antenna ports. Code division multiplexing (CDM) is used to orthogonalize the transmission on the two new virtual antenna ports, while non-orthogonal scrambling codes are introduced to support dual-layer transmission on each of the antenna ports. This new dual-layer transmission mode is targeted for beamforming schemes and supports MU-MIMO transmission for up to 4 UEs rank-1 (orthogonal) or up to 2 UEs rank-2 (non-orthogonal). However, the antenna port and scrambling code allocations are wideband, so it is not always possible to ensure orthogonality even when only 2 users are multiplexed in MU-MIMO mode. Furthermore, the only fall-back transmission mode which is supported, without mode re-configuration, is the transmit diversity. A fully adaptive SU / MU-MIMO transmission mode is not supported in LTE Release 9 but is expected to be introduced in Release 10 as described in the next section.

E. LTE-Advanced

The specifications of LTE have been extended for LTE-Advanced [17]. Although the specifications are not yet finalized several details are already in place.

Configurations with up to 8x8 MIMO antenna are to be supported and new reference signals have been introduced to support both demodulation of the downlink shared channel (DM-RS) and channel state information estimation (CSI-RS). Hence, a special attention has been given to the signaling needed for more advanced SU / MU-MIMO schemes. A new transmission mode has been defined which now includes both SU and MU-MIMO transmission capabilities without the need for the UEs to be re-configured via higher layer signaling when switching between SU and MU transmission / reception on the shared data channel [18]. This is the *transmission mode 9* (TM9).

Consequently the set of precoding codebooks has been also extended for LTE-Advanced [19]. For configuration with 2 and 4 transmit antenna the LTE-Advanced codebook is the same as the corresponding LTE codebooks. For configurations with 8 transmit antenna a dual-codebook approach is used. The precoding to be used in the dual-codebook approach is obtained via multiplication of two precoding matrices W_1 and W_2, where W_1 is block diagonal matrix matching the spatial covariance matrix of dual-polarized antenna setup and W_2 is the antenna selection and co-phasing matrix. This configuration provides good performance in both high and low spatial correlation channels. The W_1 are obtained from the coefficients of a Digital Fourier Transform (DFT) corresponding for different transmission ranks, see Table II, with details in [19].

Backwards compatibility for Release 8 and 9 UEs has been targeted. This means that many of the LTE-Advanced features and associated signaling is not visible for the Release 8 and 9 UEs and the transmission schemes defined for LTE are fully supported.

The UE feedback definition has been also extended in LTE-Advanced to account for the dual-codebook structure. When operating in a cell with 8 transmit antenna configuration the LTE-Advanced UEs are required to include in the feedback information the PMI corresponding to both W_1 and W_2. When only 2 or 4 transmit antenna are configured / used at the eNB the feedback includes only the PMI for W_2 and the W_1 is the identity matrix. Furthermore, the aperiodic CQI / PMI reporting schemes defined for LTE have been extended to support the dual-codebook [20]. The PMI for

TABLE II
CODEBOOK DESIGN IN LTE-ADVANCED FOR 8 TRANSMIT ANTENNA

Tx Rank	Beams	W_1	W_2
Rank 1-2	32	16 (per rank)	16 (per rank)
Rank 3-4	16	4 (per rank)	16 (rank 3), 8 (rank 4)
Rank 5-7	1	4	1 (per rank)
Rank 8	1	1	1 (per rank)

W_1 is always reported as a wideband PMI corresponding to the entire system bandwidth. The aperiodic feedback modes include the configurations with: wideband CQI - subband PMI W_2, wideband + 'M-preferred' CQI - wideband + 'M-preferred' PMI W_2, and subband CQI - wideband PMI W_2.

At this stage not all LTE-Advanced MIMO specifications have been finalized and there are still several open aspects to be addressed. Proposals to improve the CQI / PMI feedback also for 2 and 4 transmit antenna configurations, targeting both MU-MIMO and SU-MIMO improvement, are yet to be considered. Similar to the LTE Release 8 and 9 design principles, these further improvements have to take the performance vs. signaling overhead tradeoff into account even when utilizing the new transmission mode introduced in LTE-Advanced. The natural extensions of the RI / CQI / PMI feedback periodic and aperiodic reporting schemes already defined in LTE is to be further investigated in this context.

III. ADVANCED RECEIVER DESIGN

A. Performance / complexity trade-offs at the UE

This section highlights performance of various receivers for MU-MIMO transmission in LTE systems. Main challenges for a MU-MIMO receiver implementation include fast channel estimation and equalisation, reliable multi-user interference cancellation, and complexity issues. The detection method implemented plays a significant role in resulting performance of MU-MIMO systems and the main problem leading to the notion of infeasibility of MU-MIMO mode in LTE is the receiver structure employed by the UE being unaware of the interference created by the signal for the other UE. Although the scheduling algorithm proposed in Section II-C3 minimizes the interference based on the geometrical alignment of the channels and the precoders, the residual interference is still significant. Gaussian assumption of this significant interference and the subsequent employment of conventional single-user detectors in this scenario would be highly sub-optimal thereby leading to significant degradation in the performance.

1) Performance and Complexity Study: Maximum likelihood (ML) detection is optimal but exponentially complex as the number of antennas or the size of transmission alphabet increases. In the descending order of complexity, a number of suboptimal methods range from the successive interference cancelation (SIC) to the simple linear detectors. Non-linear algorithms, such as decision feedback based [21] or tree-based detectors [22], perform near the optimal, but still at the expense of a high complexity. Linear detectors, e.g. zero-forcing (ZF) or minimum mean square error (MMSE) criteria, are considerably less complex than ML but these detectors can suffer a significant performance loss in fading channels in particular in correlated channels [23]. Another detection method for robust LTE DL is low-complexity interference aware receiver studied in [24], [25] and references therein. These algorithms are as such readily applicable to LTE Systems.

TABLE III
BASIC LTE PARAMETERS USED IN THE SIMULATIONS

Parameters	**Setting**
Test Scenario	3GPP Macro cell case 1, 19 sites, 57 cells with 3 center cells simulated
Number of UEs	20 UEs per cell and all 20 UEs are semi-statically allocated in MU-MIMO mode when MU-MIMO transmission is configured
Carrier frequency and simulated bandwith	10 MHz bandwidth centered at 2 GHz
Packet scheduling	Proportional fair in both time and frequency domain
1st BLER target	10%
Tx and Rx	2x2 and 4x2 MIMO with SU and MU configured transmission scheme
Tx Correlation	Uncorrelated with 4 λ Tx antennas separation and 15° azimuth spread Correlated with 0.5 λ Tx antennas separation and 8° azimuth spread
MU-MIMO precoding	Unitary precoder as used in SU-MIMO LTE Release 8
MU-MIMO $CQIoffset$ applied at the eNB	-3 dB (ideal IC RX), -4.7 dB (non-IC RX)
Minimum supported data rate in MU-MIMO mode T_{min}	64 kbps
UE MU Receiver type	LMMSE, IRC and MaxLogMAP
Feedback type	Wideband Feedback (One PMI for the whole bandwidth)
Feedback delay	0 TTI and 8 TTI delay
Channel models	urban micro channel model (uncorrelated) and urban macro (correlated)

A brief performance comparison is given for interference rejection combiner (IRC) studied in [25], novel low-complexity dual stream max log MAP detector (MaxLog MAP) from [24], and low-complexity, single-user, linear MMSE detector. The effect of feedback delay, channel estimation and spatial correlation has been considered in the investigation. The downlink MU-MIMO LTE system investigated is described in Section II-C. For the link level evaluation, the parameters defined in Tab. III have been assumed. Due to the straightforward implementation Least-Squares (LS) channel estimation technique has been applied in investigation.

The results are shown in Fig. 2 - Fig. 4. Block error rate (BLER) is presented as a function of the average SNR in dB. For comparison, LTE Transmission Mode 4, SU-MIMO with the ratio of PDSCH (Physical Downlink Shared Channel) EPRE (Energy Per Resource Element) to cell-specific RS EPRE of -3dB is shown as a reference scenario.
Fig. 2 illustrates the performance of all considered detectors for QPSK 1/3, 16QAM 1/3 and 64QAM 3/4 in uncorrelated channels. As expected, the performance of the linear

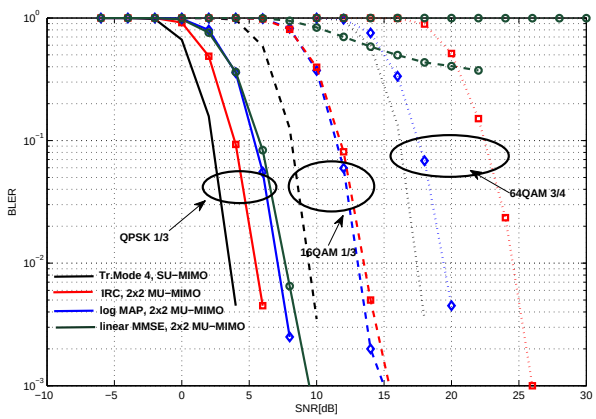

Fig. 2. BLER vs SNR[dB] performance of MU-MIMO receivers for various modulation orders, urban-micro (uncorrelated), 30km/h, no feedback delay, LS-channel estimation.

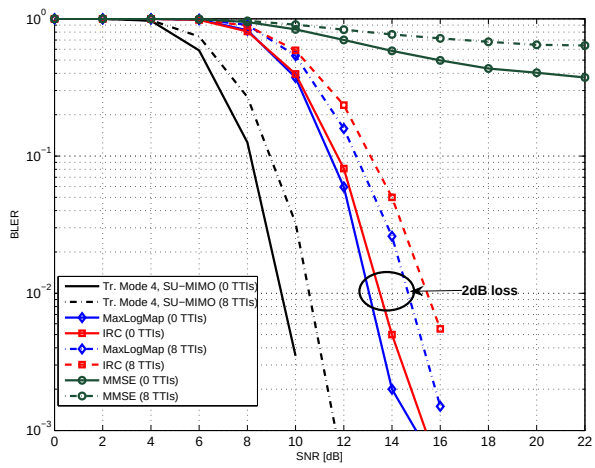

Fig. 3. BLER vs SNR[dB] performance of MU-MIMO receivers for 16QAM modulation, urban micro, 30km/h, LS- channel estimation and feedback delay.

MMSE detector degrades with increasing modulation order. For QPSK, IRC outperforms the MaxLog MAP detector. However, for 64QAM MaxLog MAP significantly outperforms IRC by almost 5dB at 10^{-2} BLER. This can be explained by the fact that MaxLog MAP detectors exploits not only the interference structure but also performs joint detection as it is aware of the modulation from the interfering user.

The joint effect of feedback delay and channel correlation is illustrated for 16QAM and interference-aware detectors in Fig. 3 and Fig. 4. In uncorrelated channels (Fig. 3), the feedback delay results in up to 2dB loss at 10^{-2} BLER. However, in the case of high channel correlation, the corresponding performance is reduced by up to 5dB at 10^{-2} BLER for feedback delay of 8 TTI's as shown in Fig. 4.

The results show that interference aware receivers are good candidates for the practical implementation in 4G systems. However, there are still certain limitations and an overall performance and complexity evaluation (more advanced channel

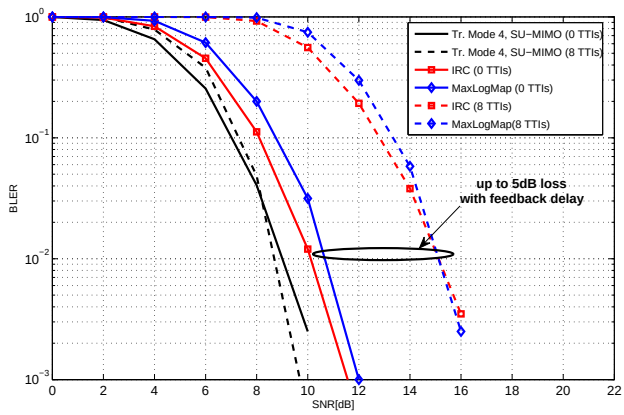

Fig. 4. BLER vs SNR[dB] performance of MU-MIMO receivers for 16QAM modulation, urban macro, 30km/h, LS- channel estimation and feedback delay.

estimator, higher number of RX antennas, UE velocity) is necessary in order to make a conclusion on the trade-offs among the selected algorithms.

B. Robust design

1) Receiver structure: Here we consider the exploitation of residual interference in the detection process rather than its Gaussian assumption and subsequent absorption in the noise. To this end, we recommend the employment of an earlier proposed low complexity interference aware receiver [24] [26] which not only reduces one complex dimension of the system but also exploits the interference structure in the detection process. Note that this interference aware receiver is independent of the dimensionality of the system and the fundamental result of the reduction of one complex dimension holds true for all dimensions. Its application to even single-antenna UEs underlines its significance as these UEs do not possess spatial degrees of freedom to cancel or attenuate the interferece via zero forcing (ZF) or MMSE filters. This low complexity receiver being based on the MF outputs and devoid of any division operation is suitable for implementation in the existing hardware [27].

However the prerequisites of this interference aware MF-based receiver are the knowledge of interference channel and its constellation. Though the proposed scheduling strategy enables the UE to find the effective interference channel (product of interference precoder and own channel) but the information regarding the interfering constellation is still eluded due to the reason that downlink control information (DCI) formats in LTE [28] do not allow the transmission of this information to the UE. The question is how much sensitive this interference aware receiver structure is to the knowledge of interfering constellation. To this end, we propose a MF-based blind receiver in Appendix which is unaware of the knowledge of the constellation of interference.

2) Link Level Simulation Results: We now look at the above-described algorithm for MU-MIMO mode in LTE Release 8 and analyze the sensitivity of this algorithm to the

knowledge of the interference constellation. For simulations, we consider the downlink of 3GPP LTE (BICM OFDM transmission) with eNB equipped with two antennas using rate-$1/3$ LTE turbo code[1] [28] with rate matching algorithm. As a reference we consider fallback transmit diversity (LTE transmission mode 2 - Alamouti code) and closed loop SU-MIMO schemes (LTE transmission mode 6) and compare them with the MU-MIMO mode (LTE transmission mode 5) employing LTE low resolution precoders. We consider ideal OFDM system (no ISI) and analyze the system in the frequency domain where the channel has *iid* Gaussian matrix entries with unit variance and is independently generated for each channel use. We assume no power control in MU-MIMO mode so two UEs have equal power distribution. For the receiver structures, we consider both single-user receiver and the low complexity MF based interference aware receiver. It is assumed that the UE knows its own channel from eNB, so in MU-MIMO mode UE can find the effective channel of interference based on the fact that eNB schedules second UE on the same RE which has requested $180°$ out of phase precoder.

To be fair from the system level perspective, we consider the case when the sum rates are equated for different transmission modes as shown in Fig. 5. In single-user modes, QAM 64 (with rate $2/3$) is served to one UE in one resource blocks (RB) while another UE is served with the same constellation in another RB so the sum rate is 4 bps/Hz. On the other hand, QAM16 (with rate $1/2$) is served to two UEs in MU-MIMO mode in both of theses two RBs so the sum rate is again 4 bps/Hz. These results amply manifest the possible gains of MU-MIMO modes in LTE when low complexity interference aware receivers are employed by the UEs alongwith the proposed scheduling strategy at the eNB. The low resolution LTE precoders being unable to completely cancel the interference underline the significance of interference aware receivers so as to exploit the structure of residual interference. Single-user detection which is based on the unrealistic assumption of Gaussianity for residual interference is highly sub-optimal in this scenario.

In Fig. 6, we look at the sensitivity of the algorithm to the knowledge of the constellation of interference for MU-MIMO mode in LTE. The simulation settings are the same except that we additionally consider the case when UE has no knowledge of the constellation of interference and it subsequently employs the blind receiver which assumes the unknown interference to be from QAM16. For comparison purposes, we also consider the cases once UE assumes the unknown interference to be from QPSK and QAM 64. The results show that there is negligible degradation in the performance of the proposed algorithm once the blind receiver is employed by the UE, i.e. assuming interference to be from QAM16 however there is significant degradation in some cases if the unknown interference is assumed to be QPSK.

It has been shown that one can obtain the best performance if the modulation of the paired UEs is known. Additional control information bits dedicated for this modulation update may not be desirable as it will increase the downlink overhead and not comparable with the current standardization. By doing a smart scheduling, it is possible to indicate what type of modulation is used for the paired UEs without having dedicated overhead bits for this purpose. The UEs are always informed which MCS will be applied to the next transmitted data packet. In the pairing and selection process we can then select or force the secondary UEs to have the same modulation as the primary one. To see how often we can actually perform the scheduling of the UE pair having the same modulation, the statistic of the scheduled MU-MIMO UEs pair with their corresponding MCSs is presented in Section IV-B.

[1]The LTE turbo decoder design was performed using the coded modulation library www.iterativesolutions.com

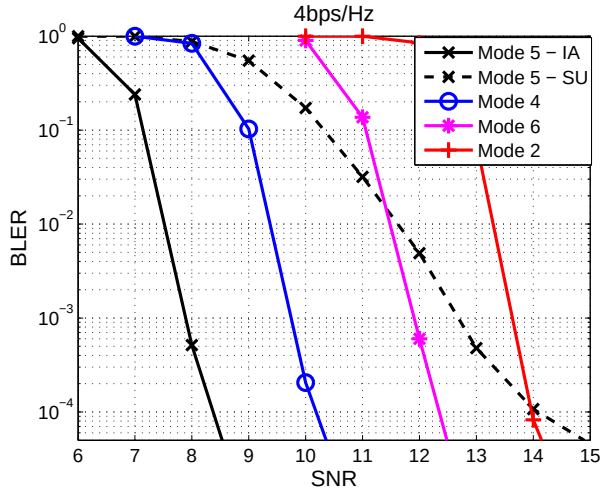

Fig. 5. Downlink fast fading channel with eNB with 2 antennas and 2 dual antenna UEs. 3GPP LTE rate $1/3$ turbo code is used with different puncturing patterns. SNR is the transmit SNR. IA indicates low complexity interference aware receiver while SU indicates single-user receiver.

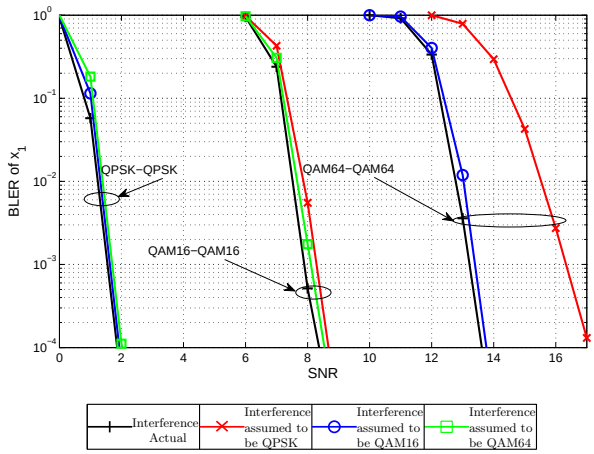

Fig. 6. Three sets of simulations are shown. QPSK-QPSK indicates that x_1 and x_2 both are QPSK. 'Interference Actual' implies the case once UE knows the constellation of interference (x_2).

IV. System level performance

A. Channel modeling

Due to its key role in system performance, the propagation channel needs to be accurately modeled. Proper correlation modeling notably is critical for MU-MIMO performance assessment. The most advanced models proposed so far are geometry-based stochastic channel models (GSCMs), like the WINNER II model [29]. These models explicitly model the geometry of the scenario by choosing random scatterer locations according to some pre-specified distribution and might incorporate large-scale fading effects into the channel realizations. When considering a complex scenario, the models inherently take antenna patterns, relative transmitter-receiver locations, angles etc. into account. Hence, the correlation matrices become truly UE-dependent and time-varying which is in accordance with measurement results. In addition, the WINNER II might account for a distance-dependent correlation between the large-scale fading parameters experienced by different terminals situated in the same geographical area.

B. Spatial MU - Packet Scheduler (MU-PS) in LTE Release 8

The packet scheduler for SU-MIMO transmission is often carried out in two phases: time domain packet scheduler (TDPS) and frequency domain packet scheduler (FDPS). An overview of this TD-FD PS framework in downlink LTE system can be found e.g. in [30], [31]. When MU-MIMO transmission scheme is configured, the UE can be scheduled in SU-MIMO (Rank 1) mode or MU-MIMO mode depending on whether the set multi-user UE pairing condition(s) is met or not. For the pairing purpose, the UEs are classified into primary UEs and candidate UEs [7]. To comply as much as possible with the SU-MIMO mode, the primary UEs are defined as the UEs scheduled for transmission using the same SU-MIMO PS mechanism. The MU-candidate UEs are all UEs with the first transmission (1st Tx). This means UEs with retransmission (2nd Tx) will not be selected as the candidate UEs. For each PRB, from the list of MU-candidates UE we try to find the best UE to pair with the primary UE. The criterion for selection is that the candidate UE should have an assigned precoder orthogonal to that of the primary UEs. This condition is applied to make sure that the UEs would not cause too much MUI to each other. To avoid scheduling the UEs at the cell-edge into MU-MIMO mode, the predicted throughput of both the primary UE and the candidate UEs at the considered PRB should be larger than a threshold T_{min}. The third requirement is that the candidate UE together with the primary UE should have the sum PF (Proportional Fair) metrics in MU mode larger than that of the primary in SU mode. Normally we have a list of candidate UEs those meet these requirements. From this list, the candidate UE that have the highest PF metric in MU mode will be finally paired with the primary UEs and set to MU transmission mode. If none of the candidate UE meets the first three requirements, the primary UE will transmit in SU mode as normal.

According to LTE Release 8 specification, the UEs are assumed to be semi-statically allocated into MU-MIMO mode. In the MU-MIMO mode (Mode 5 [12]), the current control signaling of MU-MIMO parameters is the downlink control information (DCI) format 1D. With this 1D DCI format, the UEs assume that an eNB transmission on the PDSCH would be performed on one layer [12]. There is an one additional bit to indicate the power sharing / offset and therefore imply the transmission mode of the UEs e.g. SU-MIMO mode or MU-MIMO mode. Due to this specification, the UE scheduled in the SU-MIMO will not use the rank adaptation and only be transmitted in the single stream mode.

C. Performance of LTE Release 8 MU-MIMO

Early evaluations for the LTE 2x2 MU-MIMO schemes employing various practical precoding approaches (unitary or zero-forcing) and receiver type have disclosed gains over SU-MIMO of up to 20 % only in scenarios with high transmit correlation [7]. The precoder granularity was shown to have impact mostly for low-medium transmit correlation scenarios. These conclusions have been later confirmed in general by more extensive investigations, in e.g. [3], [5], [6].

To give an idea on the performance of LTE Release 8 MU-MIMO system here we provide the system level results of 2x2 and 4x2 MU-MIMO configurations. The performances of corresponding SU-MIMO systems are also illustrated as a baseline. To comply with the Release 8 specification, the CQI / PMI feedback scheme with per subband CQI and wideband PMI as reported from the UEs was selected [12]. To make a fair comparison, this feedback scheme was applied for both the SU-MIMO and MU-MIMO transmission configurations. The major input parameters for the simulations are shown in Table III.

Figures 7 and 8 illustrate the distribution of the user throughput and the cell average throughput for 2x2 and 4x2 MIMO with SU and MU transmission configuration. It is observed that with a higher Tx correlation the performance of both SU-MIMO and MU-MIMO are better as compared with the low Tx correlation scenario. This behavior can be explained by the use of wideband PMI. In the uncorrelated Tx antennas scenario, using wideband PMI is not optimum as the fading channel varies quite a lot within the transmission bandwidth used. This leads to a degradation in the performance. On the contrary, when the Tx antennas are correlated, a single wideband PMI represents the optimal precoder for the whole transmission bandwidth. In this case, using either wideband PMI or subband PMI will not change the performance picture.

From the cumulative distribution function of the user throughput, it is observed that the 95%-ile (peak) user throughput of the MU-MIMO system is lower than that of the SU-MIMO system. At the 5%-ile (cell-edge) user throughput there is no difference in the performance of MU-MIMO system and SU-MIMO system. It is expected as in the MU-MIMO PS we try not to schedule cell-edge UEs in MU-MIMO mode Section IV-B.

For both 2x2 MIMO and 4x2 MIMO settings and in both uncorrelated and correlated Tx antennas scenarios, with full multi-user interference, the MU-MIMO system performs

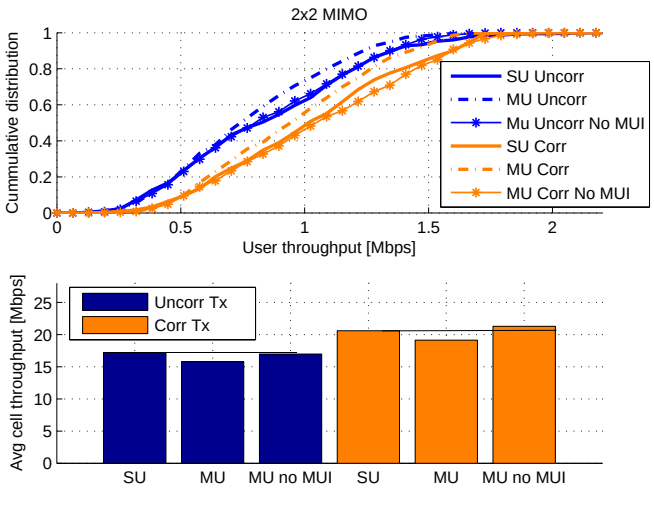

Fig. 7. Distribution of the user throughput and the average cell throughput for 2x2 MIMO setting.

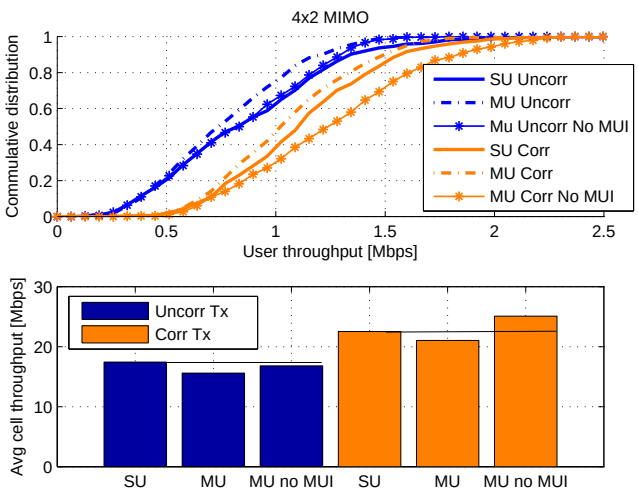

Fig. 8. Distribution of the user throughput and the average cell throughput for 4x2 MIMO setting.

worse than the SU-MIMO system with respect to the average cell throughput. Changing the Tx antenna correlation condition, from uncorrelated to correlated there is an improvement in the average cell throughput of MU-MIMO system but the enhancement is marginal. The loss in the average cell throughput for 2x2 MU-MIMO system and 4x2 MU-MIMO system as compared with the corresponding SU-MIMO system is -7% and -6% respectively.

For Release 8 UE it is possible to implement a blind receiver structure as proposed in Appendix. Fig. 6 shows that our proposed blind receiver can work well for all combinations of the modulation order of the MU-MIMO UE pairs except the 64QAM-QPSK combination. In Fig. 9 we show the statistics of the scheduled MU-MIMO UEs pair with their corresponding modulation order. It can be seen that up to 40% of the scheduled MU-MIMO pairs have the same modulation order (2-2) QPSK, (4-4) 16 QAM and (6-6) 64

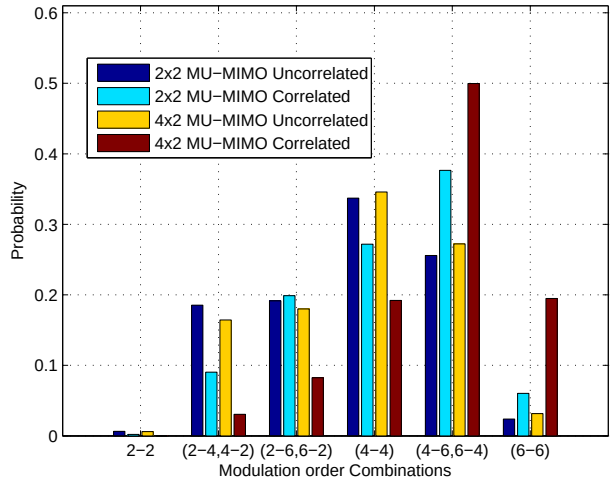

Fig. 9. Distribution of the combination of the modulation order observed at scheduled MU UEs.

QAM. In max 20% of the cases, the modulation order of the paired MU UEs is (6-2,2-6) 64QAM-QPSK. Therefore, without significantly reducing the number of MU UEs, we can safely avoid scheduling the candidate UE which together with the primary UE having this combination of the modulation order .

Based on these observations, we further assume a perfect interference canceling algorithm as upper bound for the practical performance of the blind receiver structure as proposed in Appendix. Figures 7 and 8 show the system level results obtained under these receiver assumptions. In uncorrelated Tx scenario, even with perfect multi user interference cancelation, the performance of MU-MIMO system is inferior to that of the SU-MIMO system. This indicates that one should not use MU-MIMO in a uncorrelated Tx scenario. In a correlated Tx scenario, 2x2 MU-MIMO system and 4x2 MU-MIMO system obtain a gain in the average cell throughput of 3% and 11% respectively.

The CQI / PMI feedback scheme used for the results presented in Figures 7 and 8 was limited to the specifications of LTE Release 8. More features are now investigated and proposed in LTE-Advanced standardization, which can facilitate the optimal MU-MIMO transmission and reception. The next section explores some of the potential improvements to be introduced.

D. LTE-Advanced enhancements

Specific CQI and PMI: Using the SU-MIMO codebook for MU-MIMO transmission may not fully utilize the multi-user diversity. This is because the SU-MIMO codebook are designed to optimize the performance of a single-user while the additional degree of freedom in the spatial domain one can obtain in the MU-MIMO transmission is not fully taken into consideration. Therefore it could be beneficial if there is

a separated codebook designed specifically for MU-MIMO transmission mode. The multi-granular precoder is expected to boost the performance of MU-MIMO system performance as described in [32], [33], [34]. Of course this could raise the concern on the increase feedback overhead once an additional MU-MIMO precoder need to be feedback be the UE in parallel with the normal SU-MIMO precoder. Another proposed solution is to report the CQI / PMI separately for SU-MIMO and MU-MIMO transmission [35], [36]. In additional to the normal SU CQI / PMI feedback, UE capable of receiving MU-MIMO reception could report an additional best companion UE PMI and the expected CQI with that setting. To reduce the feedback overhead, only the difference (delta) between the MU-CQI and SU-CQI is feedback as extra information. These schemes allow for a dynamic switching between SU and MU mode. One of the drawbacks of these types of proposals is that more feedback overhead is introduced. Moreover, if the paired UEs are restricted to have the same precoding as the best companion precoding then the number of potential UEs available for pairing at the eNB will be very limited. This could significantly reduce the number of UEs scheduled in MU-MIMO mode and thereby prohibit cell level the performance gain from using MU-MIMO transmission.

Link adaptation and scheduling: Although the outer loop link adaptation (OLLA) [37], [38] can help to adjust the estimated MCS for SU-MIMO and compensate for systematic CQI estimation errors, for MU-MIMO in particular, the mismatch between the estimated MU-MIMO CQI and the true channell CQI could still significantly degrade the system performance. For example the mismatch in the estimated MU-MIMO CQI could lead to a wrong MU-MIMO pairing decision as well as incorrect assignment of the modulation and coding scheme (MSC). However, as the UE has no knowledge of the other UE it will be paired with, it is a challenge to estimate the MU-MIMO CQI with a high degree of accuracy. Currently the most common way of estimating the MU-MIMO CQI is to estimate it from the single stream SU-MIMO CQI reported by the UE with some offset. Particularly for 2x2 MU-MIMO, the offset is around 4.7 dB to account for the power sharing of the two UEs scheduled on the same PRB and the MU interference. The offset value should be differently set for different transmission schemes e.g. orthogonal unitary precoder or ZF. This is because the unitary precoder is already normalized so that it has norm one. The difference between the SU-MIMO and MU-MIMO comes mainly from the transmission power to the UE in each mode and the MU interference. Meanwhile for ZF, the mismatch between the estimates of MU-MIMO CQI also comes from another fact that the precoder used in the estimation of the SU-MIMO CQI at the UE side is totally different from the actually used transmit ZF precoder at the eNB side.

With the introduction of the DM-RS in LTE-Advanced, as the multi-user precoded signals can be estimated at the UE it is possible to implement a more performing LMMSE receiver with a better multi-user interference covariance matrix estimation.

MU-MIMO scheduling is dependent very much on how much information on the channel can be feedback by the UEs to the serving eNB. There is therefore trade off in the performance improvement and the feedback overhead. Currently in LTE Release 8 the UEs are semi-statically allocated to MU-MIMO mode. It means, the UE can not switch from MU-MIMO transmission configuration to SU-MIMO (Rank > 1) transmission configuration between subframe. As mentioned in Section IV-B, together with the specified DCI format these rules limit the UE comparability in using rank adaptation when it is not scheduled in MU-MIMO mode. This issue is expected to be solved in LTE-Advanced when a additional transmission mode, Mode 9 and new DCI format is introduced. This mode would allow for a dynamic switching between SU-MIMO and MU-MIMO and support a SU-MIMO up to rank 8 [18].

V. Conclusions

This article first provides a detailed overview of the MU-MIMO schemes encountered in 3GPP standardization: from a unique mode in LTE Release 8 to more advanced possibilities offered by LTE-Advanced. Moreover, a new scheduling algorithm based on the geometrical alignment of interference at the base station is proposed. This algorithm relegates the effective interference seen by each user equipment.

Various receiver structures are then studied. Their performance is assessed in different scenarios thanks to link level simulations. Besides classical schemes, an interference aware receiver showing appealing performance gains is studied.

System level simulations for LTE Release 8 are presented and analyzed. It is notably highlighted that both for SU-MIMO and MU-MIMO scenarios better performance is obtained in scenarios with higher Tx correlation than scenarios with low Tx correlation. Interestingly, it is also shown that in terms of average cell throughput, MU-MIMO offers superior performance with respect to SU-MIMO only in correlated scenarios. Furthermore, this gain is shown to be marginal. This disappointing result originates from the limited MU-MIMO features included in Release 8. Hence, proposals considered in LTE-Advanced standardization to better exploit the MU-MIMO potential are thus discussed. They consist in MU specific CQI and PMI as well as enhanced link adaptation and scheduling.

Acknowledgments

The research work leading to this article has been partially funded by the European Commission under FP7 SAMURAI project. Further details can be found in http://www.ict-samurai.eu/.

APPENDIX

We propose a blind receiver where UE does not know the interfering constellation. The max log MAP bit metric for bit b of x_1 is given as [39]

$$\Lambda_1^i\left(y_1,b\right)\approx\min_{x_1\in\chi_{1,b}^i,x_2\in\chi_2}\left|y_1-\mathbf{h}_1^\dagger\mathbf{p}_1x_1-\mathbf{h}_1^\dagger\mathbf{p}_2x_2\right|^2, \quad (3)$$

where $\chi_{1,b}^i$ denotes the subset of the signal set $x_1\in\chi_1$ whose labels have the value $b\in\{0,1\}$ in the position i. We now expand the bit metric which can be rewritten as

$$\Lambda_1^i\left(y_1,b\right)\approx\min_{x_1\in\chi_{1,b}^i,x_2\in\chi_2}\left\{\left|\mathbf{h}_1^\dagger\mathbf{p}_1x_1\right|^2-2\left(y_{1,MF}x_1^*\right)_R\right.$$
$$\left.+\left|\mathbf{h}_1^\dagger\mathbf{p}_2\right|^2x_{2,R}^2-2\left|\psi_A\right|\left|x_{2,R}\right|+\left|\mathbf{h}_1^\dagger\mathbf{p}_2\right|^2x_{2,I}^2-2\left|\psi_B\right|\left|x_{2,I}\right|\right\}, \quad (4)$$

where $y_{1,MF}=y_1\left(\mathbf{h}_1^\dagger\mathbf{p}_1\right)^*$ and $y_{2,MF}=y_1\left(\mathbf{h}_1^\dagger\mathbf{p}_2\right)^*$ are the outputs of MF. Note that subscripts $(.)_R$ and $(.)_I$ indicate real and imaginary parts respectvely. We have introduced two more notations which are given as

$$\psi_A=p_{12,R}x_{1,R}+p_{12,I}x_{1,I}-y_{2,MF,R}$$
$$\psi_B=p_{12,R}x_{1,I}-p_{12,I}x_{1,R}-y_{2,MF,I},$$

where $\rho_{12}=\left(\mathbf{h}_1^\dagger\mathbf{p}_1\right)^*\mathbf{h}_1^\dagger\mathbf{p}_2$ is the cross correlation between the two coefficients. For the minimization of the bit metric, the values of $x_{2,R}$ and $x_{2,I}$ need to be in the opposite directions of ψ_A and ψ_B which explains the terms $-2\left|\psi_A\right|\left|x_{2,R}\right|$ and $-2\left|\psi_B\right|\left|x_{2,I}\right|$.

UE needs to know the constellation of x_2 to compute (4). Here we propose that UE assumes interference (x_2) to be from QAM16. As LTE specifications [15] include only three constellations i.e. QPSK, QAM16 and QAM64, so assuming interference to be from QAM16 is a reasonable compromise. It would not only capture the effect of four quadrants of QPSK constellation points but will also encapsulate the spread of QAM64 constellation points in each quadrant. As the values of $x_{2,R}$ and $x_{2,I}$ for the case of QAM16 are $\left[\pm\frac{\sigma_2}{\sqrt{10}}\ \pm\frac{3\sigma_2}{\sqrt{10}}\right]$ so the magnitudes of $x_{2,R}$ and $x_{2,I}$ which minimize the bit metric (4) are given as

$$\left|x_{2,R}\right|=\sigma_2\frac{1}{\sqrt{10}}\left(2+(-1)^{I\left(\left|\psi_A\right|<\sigma_2\frac{2\left|\mathbf{h}_1^\dagger\mathbf{p}_2\right|^2}{\sqrt{10}}\right)}\right) \quad (5)$$

$$\left|x_{2,I}\right|=\sigma_2\frac{1}{\sqrt{10}}\left(2+(-1)^{I\left(\left|\psi_B\right|<\sigma_2\frac{2\left|\mathbf{h}_1^\dagger\mathbf{p}_2\right|^2}{\sqrt{10}}\right)}\right) \quad (6)$$

and $I\left(.\right)$ is the indicator function defined as

$$I\left(a<b\right)=\begin{cases}1 & \text{if } a<b\\ 0 & \text{otherwise.}\end{cases}$$

So the bit metric for blind receiver is written as:

$$\Lambda_1^i\left(y_1,c_{k'}\right)\approx\min_{x_1\in\chi_{1,c_{k'}}^i}\left\{\left|\mathbf{h}_1^\dagger\mathbf{p}_1x_1\right|^2-2\left(y_{1,MF}x_1^*\right)_R\right.$$
$$\left.-2\left|\psi_A\right|\left|x_{2,R}\right|+\left|\mathbf{h}_1^\dagger\mathbf{p}_2\right|^2\left|x_{2,R}\right|^2-2\left|\psi_B\right|\left|x_{2,I}\right|+\left|\mathbf{h}_1^\dagger\mathbf{p}_2\right|^2\left|x_{2,I}\right|^2\right\}$$

where $\left|x_{2,R}\right|$ and $\left|x_{2,I}\right|$ are given by (5) and (6).

REFERENCES

[1] Finnish Communications Regulatory Authority, "Ficora Traffic Report for 1H/2010," http://www.ficora.fi/attachments/5tPwk2SWH/Markkinakatsaus_3_2010_-_Puolivuosikatsaus.pdf, March 2010.

[2] Cisco VNI Forecast,"Cisco Visual Networking Index: Global Mobile data Traffic Forecast Update 2009-2014," Cisco Public Information, February 9, 2010.

[3] A. Ghosh et al., "LTE-Advanced: Next-Generation WIreless Boradband Technology," *IEEE Wireless Comm. Mag.*, June 2008, pp. 10-22.

[4] Q. Li et al., "MIMO techniques in WiMAX and LTE: A feature Overview," *IEEE Comm. Mag.*, May 2010, pp. 86-91.

[5] K. Kusume et al., "System Level performance of Downlink MU-MIMO Transmission for 3GPP LTE-Advanced," *Proc. IEEE Veh. Tech. Conference (VTC-Fall)*, Ottawa, Canada, Sept. 2010.

[6] A. Farajidana et al.,"3GPP LTE Downlink System Performance," *Proc. IEEE Global Communications Conference (Globecomm)*, Honolulu, Hawaii, USA, Nov.-Dec. 2009.

[7] C.B. Ribeiro et al., "Performance of Linear Multi-User MIMO Precoding in LTE System," *Proc. Int. Symp. on Wireless Pervasive Computing (ISWPC)*, Santorini, Greece, May 2008.

[8] I.Z. Kovacs et al., "Toward a Reconfigurable MIMO Downlink Air Interface and Radio Resource Management: The SURFACE Concept," *IEEE Comm. Mag.*, June 2010, pp. 22-29.

[9] G. Caire and S. Shamai, "On the achievable throughput of a multiantenna Gaussian broadcast channel", *IEEE Transactions on Information Theory*, vol.49, no.7, pp. 1691-1706, July 2003.

[10] Q.H. Spencer, A.L. Swindlehurst, and M. Haardt, "Zero-forcing methods for downlink spatial multiplexing in multiuser MIMO channels," *IEEE Transactions on Signal Processing*, vol.52, no.2, pp. 461-471, Feb. 2004.

[11] C.B. Peel, B.M. Hochwald and A.L. Swindlehurst, "A vector-perturbation technique for near-capacity multiantenna multiuser communication-part I: channel inversion and regularization," *IEEE Transactions on Communications*, vol.53, no.1, pp. 195-202, Jan. 2005.

[12] 3GPP Technical Specification Group Radio Access Network; Evolved Universal Terrestrial Radio Access (E-UTRA); "Physical Layer Procedures (Release 9)" 3GPP TS36.213 V9.3.0, June 2010.

[13] 3GPP Technical Specification Group Radio Access Network; Evolved Universal Terrestrial Radio Access (E-UTRA); "Physical Channels and Modulation (Release 9)" 3GPP TS36.211 V9.1.0, March 2010.

[14] 3GPP Technical Specification Group Radio Access Network; "Requirements for Evolved UTRA (E-UTRA)and Evolved UTRAN (E-UTRAN) (Release 7)," 3GPP TR25.913 V7.3.0, March 2006.

[15] 3GPP TS 36.211, "Evolved Universal Terrestrial Radio Access (E-UTRA); Physical Channels and Modulation, Release 8, V.8.6.0," 2009.

[16] S. Sesia, I. Toufik and M. Baker, "LTE, The UMTS Long Term Evolution: From Theory to Practice," Wiley, 2009.

[17] 3GPP Technical Specification Group Radio Access Network; Evolved Universal Terrestrial Radio Access (E-UTRA); "Further advancements for E-UTRA physical layer aspects (Release 9)," 3GPP TR36.814 V9.0.0, March 2010.

[18] 3GPP TSG RAN WG1 #62, "Way Forward on Transmission Mode and DCI design for Rel-10 Enhanced Multiple Antenna Transmission," R1-105057, Madrid, Spain, August 2010.

[19] 3GPP TSG RAN WG1 #62, "Way forward on 8 Tx Codebook for Release 10 DL MIMO," R1-105011, Madrid, Spain, August 2010.

[20] 3GPP TSG RAN WG1 #62, "Way Forward on Aperiodic PUSCH CQI modes in Release 10," R1-105058, Madrid, Spain, August 2010.

[21] Foschini GJ, Golden GD, Valenzuela RA, Wolniansky PW. Simplified processing for high spectral efficiency wireless communication employing multi-element arrays. IEEE Journal on Selected Areas in Communications, vol. 17; pp. 1841-1852. 1999;

[22] Jong YLC, Willink TJ. Iterative tree search detection for MIMO wireless systems. Proceedings of IEEE 56th, Vehicular Technology Conference, Vancouver, Canada, September 2002; 1041-1045.

[23] H. Artes, D. Seethaler, F. Hlawatsch, "Efficient detection algorithms for MIMO channels: a geometrical approach to approximate ML detection," *IEEE Trans. Signal Process*, vol. 51, no.11, pp. 2808-2820, Nov. 2003.

[24] R. Ghaffar and R. Knopp, "Interference Suppression for Next Generation Wireless Systems," *IEEE 69-th Vehicular Technology Conference VTC-Spring 2009* , Barcelona, Apr. 2009.

[25] Wireless World Initiative New Radio WINNER Project, "D1.4 Initial Report on Advanced Multiple Antenna Systems," D1.4, Jan. 2009.

[26] R. Ghaffar and R. Knopp, "Linear Precoders for Multiuser MIMO for finite constellations and a simplified receiver structure under controlled interferenc," *Asilomar Conference on Signals, Systems and Computers* , Pacific Grove, USA, Nov. 2009.

[27] R. Ghaffar and R.Knopp, "Low Complexity Metrics for BICM SISO and MIMO Systems," *Proc. IEEE Veh. Tech. Conference (VTC-Spring)*, Taipei, Taiwan, May 2010.

[28] 3GPP TS 36.212, "Evolved Universal Terrestrial Radio Access (E-UTRA); Channel Coding and Multiplexing, Release 8, V.8.6.0," 2009.

[29] P. Kyösti *et al.*, "WINNER II Channel Models," ver. 1.1, Sept. 2007. Available: http://www.ist-winner.org/WINNER2-Deliverables/D1.1.2v1.1.pdf.

[30] A. Pokhariyal, K.I. Pedersen, G. Monghal, I.Z. Kovacs, C. Rosa, T.E. Kolding, P.E. Mogensen, "HARQ Aware Frequency Domain Packet Scheduler with Different Degrees of Fairness for the UTRAN Long Term Evolution," *Proc. IEEE Veh. Tech. Conference (VTC-Spring)*, Dublin, Ireland, April 2007.

[31] G. Monghal, K.I. Pedersen, I.Z. Kovacs, P.E. Mogensen, "QoS Oriented Time and Frequency Domain Packet Schedulers for The UTRAN Long Term Evolution," *Proc. IEEE Veh. Tech. Conference (VTC-Spring)*, Singapore, May 2008.

[32] R1-103480 3GPP TSG RAN WG1 #61Bis "Multi-granularity codebooks for 4Tx DL MIMO".

[33] R1-103449 3GPP TSG RAN WG1 meeting #61bis "Double codebook based Differential feedback for MU-MIMO enhancement".

[34] R1-103703 3GPP TSG RAN WG1 #61bis "System-Level Evaluation Results on 8Tx Codebook".

[35] R1-092680 3GPP TSG RAN WG1 #62 Meeting "Further analysis of companion feedback performance and feedback signalling overhead reduction".

[36] R1-090926 3GPP TSG RAN WG1 #56 Meeting "Best Companion reporting for improved single-cell MU-MIMO pairing".

[37] H.Holma, A.Toskala "LTE for UMTS - OFDMA and SC-FDMA Based Radio Access," ISBN: 978-0-470-99401-6.

[38] K.I. Pedersen et al. , "Frequency Domain Scheduling for OFDMA with Limited and Noisy Channel Feedback," *Proc. IEEE Veh. Tech. Conference (VTC-Fall)*, Baltimore, USA, Sept.-Oct. 2007.

[39] G. Caire, G. Taricco, and E. Biglieri, "Bit-interleaved coded modulation," *IEEE Transactions on Information Theory*, vol.44, no.3, pp.927-946, May 1998.